1975

Computer Generated Holograms

Jeffrey James Gierloff
University of Central Florida

COMPUTER GENERATED HOLOGRAMS

BY

JEFFREY JAMES GIERLOFF
B.S., University of Minnesota, 1968

RESEARCH REPORT

Submitted in partial fulfillment of the requirements
for the degree of Master of Science
in the Graduate Studies Program of
Florida Technological University

Orlando, Fla.
1975

TABLE OF CONTENTS

LIST OF ILLUSTRATIONS

ACKNOWLEDGMENTS

I wish to thank Dr. R. L. Phillips of Florida Technological University for his assistance with the technical aspects of the paper. I also appreciate the cooperation of the management of the Florida Research and Development Center for allowing use of their computer and optical facilities.

INTRODUCTION

Computer generated holograms have been made practical by the introduction of fast Fourier transform alogrithms. The following discussion will brief the reader on the theory and concepts of optical holograms, the computer hologram, and the analogies of the computer hologram to its optical counterpart. Some of the programming aspects of the computer holograms are presented. The results of the generation of several computer holograms are presented, and conclusions drawn as to the effectiveness of this technique. Finally, some of the practical uses and advantages of the computer hologram are discussed.

CHAPTER I

DESCRIPTION OF A FRESNEL HOLOGRAM

A hologram is a record on a photographic film transparency of the phase and amplitude information from an object. This is accomplished by interfering coherent light from the object with light from a reference source. The resulting interference pattern is then recorded on photographic film.

A typical Fresnel holographic setup is illustrated in Figure 1a. A coherent, monochromatic, nondiverging beam of light is incident upon a beam splitter, which reflects part of the beam onto the object and transmits the unaltered remainder of the beam onto the photographic film. The light reflected off of the object, called the object wave, now had its amplitude and phase altered due to its interaction with the object. The object wave and reference wave form an interference pattern which is recorded on the photographic plate. To retrieve the image from the hologram, a plane wave is directed through the hologram. The diffraction pattern formed is the reconstruction of the object wave, as shown in Figure 1b. A real image is also formed. The important feature of this arrangement is the total coherence of the light produced by the laser source, where coherence means that the phase and intensity at a given point on the wave is

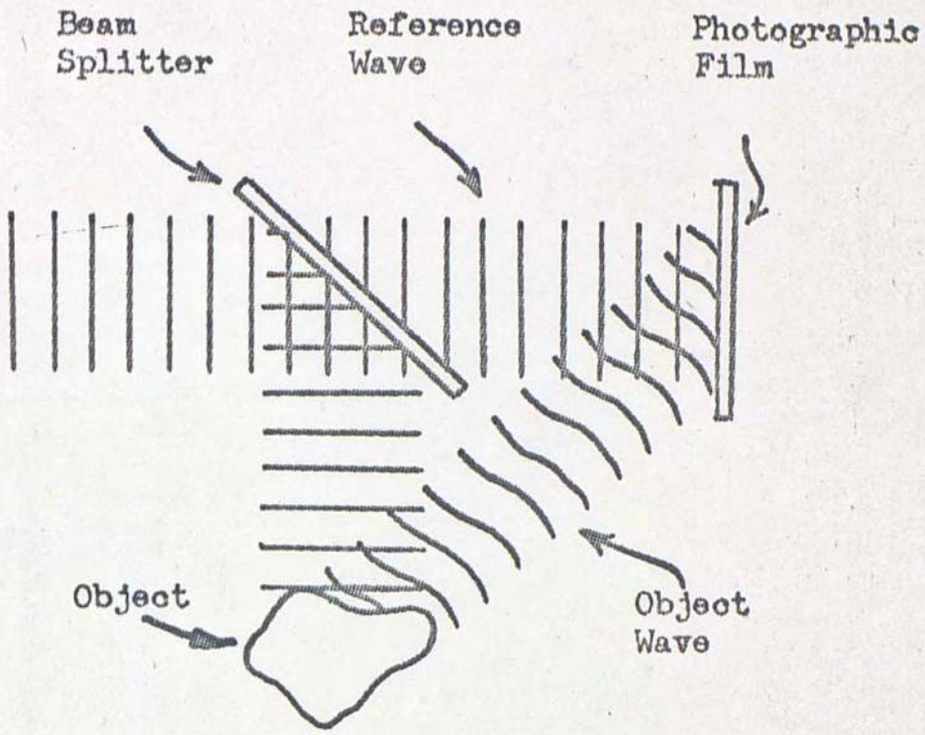

a. Optical Generation of Hologram

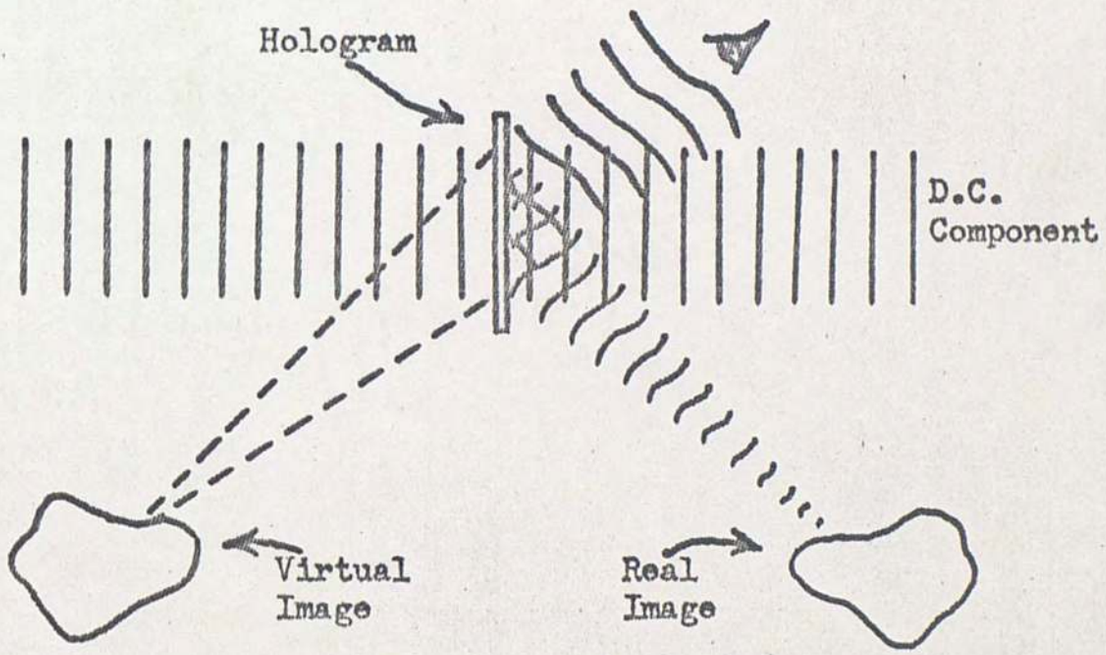

b. Optical Reconstruction of Waveform

FIGURE 1: OPTICAL GENERATION OF FRESNEL HOLOGRAMS

constant relative to any other point on the wave for all time. Because of this it is conceptually easier to think of the optical wave as being "frozen in time", due to the unchanging amplitude and phase relationships.

Accordingly, useful equations for optical waves may be written that are independent of time. A monochromatic coherent wave may be written as

$$u(x,y,z) = U(x,y)\exp(-j2\pi\frac{z}{\lambda} + \phi(x,y)) \qquad (1)$$

where

λ is the wavelength of the light,

ϕ is the phase

z is the coordinate in the direction of propagation,

x,y are the coordinates normal to the direction of propagation,

U is the amplitude variation along the wavefront.

A monochromatic coherent plane wave with constant phase and amplitude may be written as

$$u(z) = K\exp(-j2\pi\frac{z}{\lambda}) \qquad (2)$$

A plane wave incident at an angle onto a flat surface has an amplitude on the surface expressed as

$$u(x') = K\exp(-j2\pi\frac{x'}{\ell}) \qquad (3)$$

at a given instant of time, where ℓ is the length between points of equal phase on the flat surface and x' is the direction on the flat surface parallel to the plane of the paper, as illustrated in Figure 2. Assuming a small angle θ

$$\frac{x}{f} = \frac{\lambda}{\ell}$$

$$\frac{\Delta x}{f} \approx \frac{\lambda}{\ell}$$

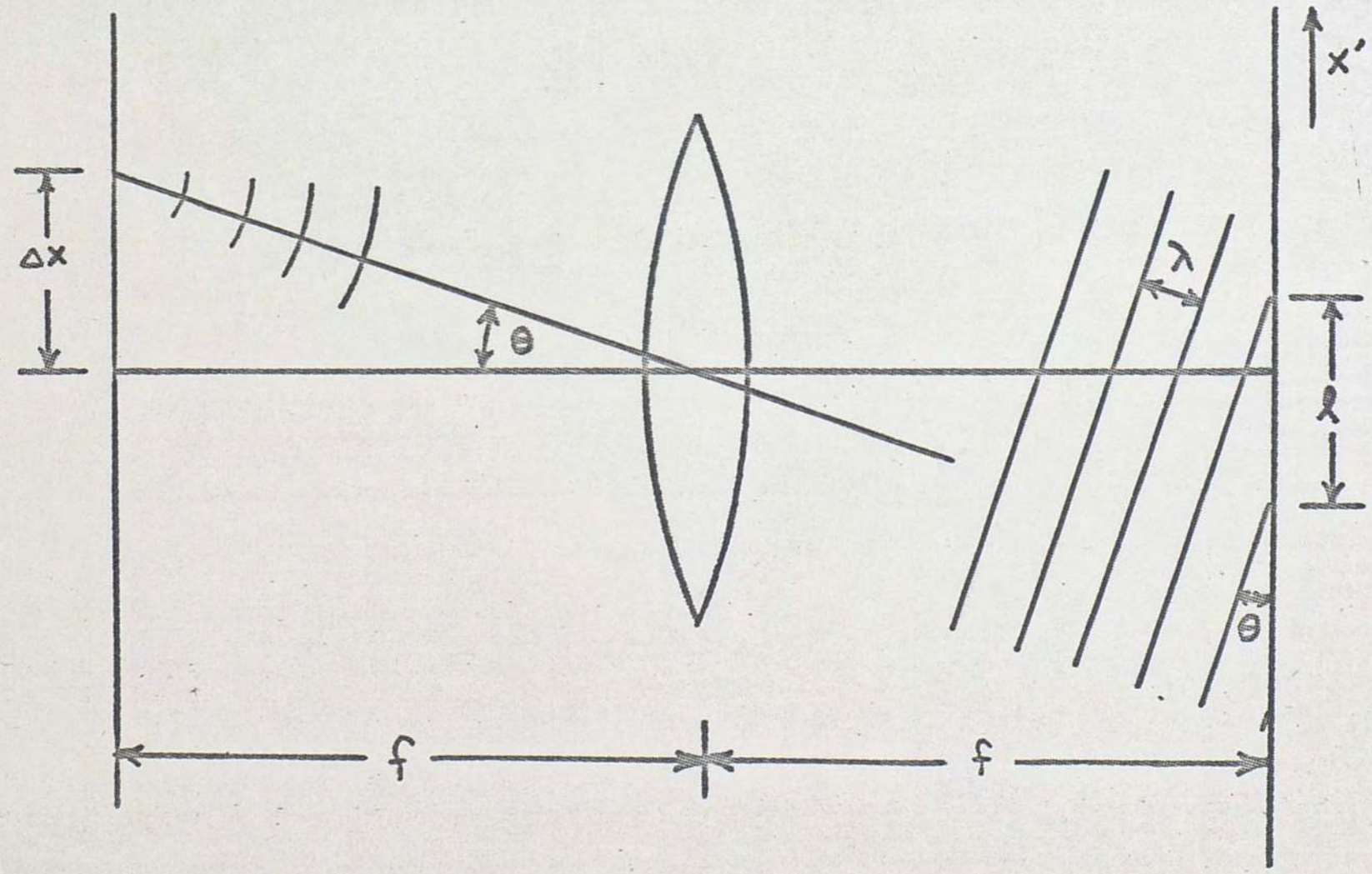

FIGURE 2: PLANE WAVE INCIDENT ON A FLAT SURFACE

and

$$\ell \approx \frac{\lambda f}{\Delta x} \tag{4}$$

so that the amplitude of a plane wave incident on a flat surface may be expressed as

$$u(x') = K \exp\left(-j\frac{2\pi x'\Delta x}{\lambda f}\right) \tag{5a}$$

or as

$$u(\nu) = K \exp\left(-j2\pi\nu\Delta x\right) \tag{5b}$$

if $\nu \triangleq \frac{x'}{\lambda f}$ is the spatial frquency.

If the plane wave is considered the reference wave and the object wave is also a plane wave propagating parallel to the z-axis, the resulting interference pattern will be a series of alternating dark and bright lines. For example, in Figure 2, if the object wave front happened to coincide with the flat surface at the instant that these wavefronts were viewed, we would then have the highest intensity at the points where the two wave fronts meet. In Figure 2, these would be parallel bright lines perpendicular to the plane of the paper. The value of the concept of two undistorted interfering plane waves will be obvious when the format of the computer generated hologram is discussed.

The Fresnel hologram is a familiar hologram to most people, such holograms are being used for general viewing purposes demonstrating 3-D effects. The computer holograms generated are not Fresnel holograms but Fourier holograms. The Fresnel hologram is an easier hologram to understand and serves as a useful introduction to the Fourier hologram and to the computer generated hologram.

CHAPTER II

DESCRIPTION OF A FOURIER HOLOGRAM

The optical configuration for a Fourier hologram is illustrated in Figure 3. A collimated monochromatic coherent beam of light falls on a pinhole and on a photographic transparency. The light emerges from the pinhole with spherical wavefronts, which are then collimated by a lens into plane waves. These plane waves form the reference beam and are identical to the reference beam in the Fresnel hologram. Note that the lens effectively puts the pinhole reference point source at infinity with respect to the photographic film, since the pinhole is at the focal length of the lens. While the pinhole and lens combination is easy to understand, the effect that the lens has on the object wave is not. First consider that while the transparency will have an effect on the amplitude and phase of the incident plane wave, the emerging object wave will still nearly be a plane wave. Because of this and the fact that the photographic film is located at the focal length of the lens, the object wave is essentially focussed down to a spot. It isn't quite focussed to a point because of effects caused by the finite object size and the amplitude and phase variations introduced into the plane wave by the object.

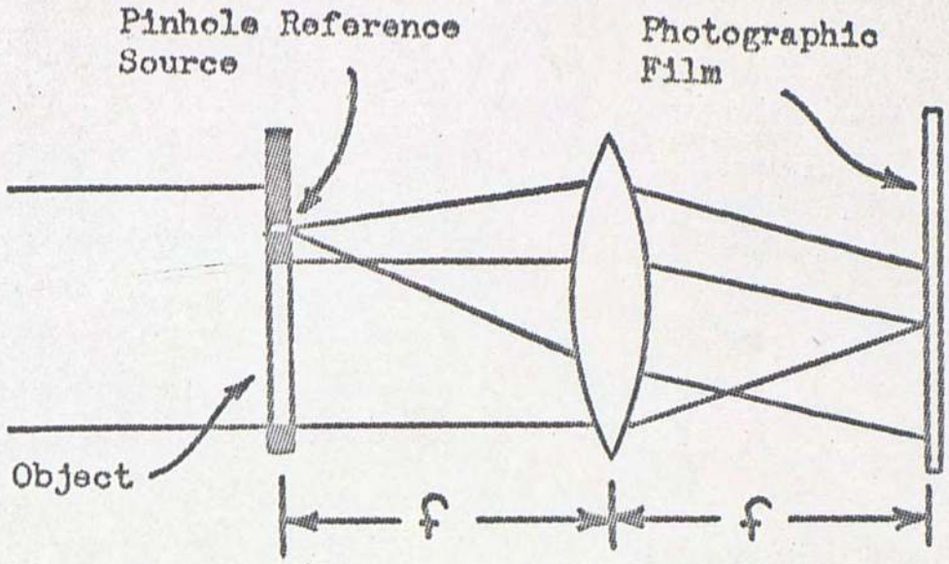

a. Optical Generation of Hologram

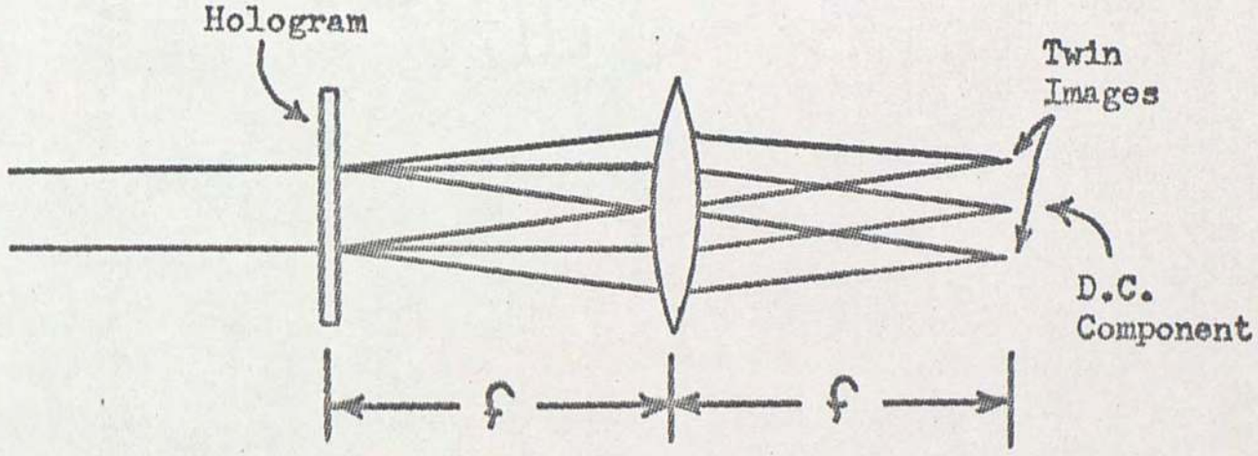

b. Reconstruction of Waveform

FIGURE 3: OPTICAL GENERATION OF FOURIER HOLOGRAMS

The normalized mathematical expression for the amplitude at the spot is given by

$$\tilde{u}(\nu,\mu) = \iint u(x,y)\exp(-2\pi j(x\nu + y\mu)dxdy \qquad (6)$$

where

$$\nu = \frac{x'}{\lambda f} \text{ and } \mu = \frac{y'}{\lambda f}$$

and where

x,y are the coordinates in the object plane,

ν,μ are the frequency coordinates in the film plane,

u(x,y) represents object amplitude and phase characteristics,

$\tilde{u}(\nu,\mu)$ represents image amplitude and phase characteristics.

Equation 6 states that the image $\tilde{u}(\nu,\mu)$ is the two dimensional Fourier transform of the object. Both u(x,y) and $\tilde{u}(\nu,\mu)$ are in general complex functions. For the particular case used here, the object u(x,y) will not be complex, since it will only have amplitude variations. The image $\tilde{u}(\nu,\mu)$ will still be complex, however. So the lens produces an image that is the two dimensional Fourier transform of the object. It also effectively puts the object an infinite distance away from the film. This is easy to see if a point on the object is considered. It would transmit light just as the pinhole would. Because of the lens, the pinhole appears to be located at infinity, and so will each point on the object. Because the object appears to be at infinity, three dimensional effects are not possible with this configuration. However a slightly more elaborate configuration can be used for three dimensional effects.

Figure 3b illustrates the optical process used to retrieve the object wave from the hologram. It is similar to the process used for the Fresnel hologram. A plane wave is incident on the hologram and produces two twin images and a "zero order" component. A lens may then be used to form the Fourier transform of the wavefronts producing the original image duplicated around a D.C. component which is the undisturbed potion of the reference wave.

CHAPTER III

THE COMPUTER HOLOGRAM

A computer generated hologram uses the Fourier hologram configuration rather than the Fresnel hologram configuration for two basic reasons. First, and most important, is the question of physical size. Both holograms diffract light. In order to do so the basic intensity variations on the holograms must have a spacing on the order of a wavelength of light. This is illustrated in Figure 2. However, most of the interference pattern is centered around small central spot for a Fourier hologram while it is spread over a large area for a Fresnel hologram. The central spot could have dimensions of a millimeter for the Fourier hologram. The Fresnel hologram could have dimensions of 100 millimeters for convenient viewing. For this example the difference in area is 10,000 times. Very small variations spread over a large area means a very large number of computations and high cost of computer time. The Fourier transform is formed in such a way as to facilitate formation of the image in spite of its small size. The second reason is that the mathematical formulation for the Fourier transform is easier to work with than the Fresnel transform.

As an example of the dimensions required for a Fourier hologram, consider the following conditions:

$\lambda = 6328$ Å

$\Delta x = 6.4$ cm

$\delta x = 0.1$ cm

$f = 100$ cm

where λ is the wavelength of the coherent radiation,

Δx is the spacing of the pinhole reference,

δx is the smallest resolution spacing in the object,

f is the focal length of the lens.

Then the average fringe spacing is

$$\ell \approx \frac{\lambda f}{\Delta x} = \frac{(6328 \times 10^{-8}\text{cm})(100\text{cm})}{6.4\text{ cm}} \approx 0.01\text{ mm} \qquad (7)$$

If the smallest resolution spacing is 0.1 cm, the highest frequency component is located at

$$x' = \frac{\lambda f}{\delta x} = \frac{(6328 \times 10^{-8}\text{cm})(100\text{cm})}{0.1\text{ cm}} \approx 0.64\text{ mm} \qquad (8)$$

This can eaily be visualized by considering Figure 2 as being the result of two elements in the object separated by the minimum resolution spacing. After passing through a lens located one focal length from the object, the two spherical fronts are Fourier transformed into two plane wave fronts as shown in Figure 2. The basic pattern repetition rate will correspond to the length ℓ of Figure 2, which is called $\Delta x'$ in equation 8. How does this sound physically? If 64 elements could be resolved in the x direction on one side of the object, a maximum of 64 fringes would then

be required to be resolved on one side of the hologram.

Since a computer program deals with discrete functions, we must replace equation 6 with a digital form (Lohmann 1965).

$$u(n,m) = \sum_{i,j=0}^{N-1} u(i,j) \exp(-2\pi j(in + jm)/N) \qquad (9)$$

where

i,j are the indices of the object array,

n,m are the indices of the image array,

N is the number of elements in each dimension of the array.

This equation as it stands would require N^2 operations per point. For a 64 X 64 array this amounts to N^4 operations or 16.8×10^6 operations for the hologram. James Cooley and John Tukey (1965) arrived at a more efficient method of computation for equation 9, commonly known as either the Cooley - Tukey Alogrithm or as the Fast Fourier Transform (FFT). The Fast Fourier Transform reduces the number of operations from a total of M^2,

$M = N^2$, the total number of points,

to $2M\log_2 M$ operations. This amounts to 68139 operations for a 64 X 64 array or roughly 250 times faster. The computational time improvement is presented in Figure 4. An excellent discussion of digitized Fast Fourier Transforms is covered in Digital Processing of Signals by Gold.

The basic mathematical generation of a Fourier computer generated hologram is illustrated in Figure 5. The indices in equation 9 run from 0 to N-1, implying that the range of integration

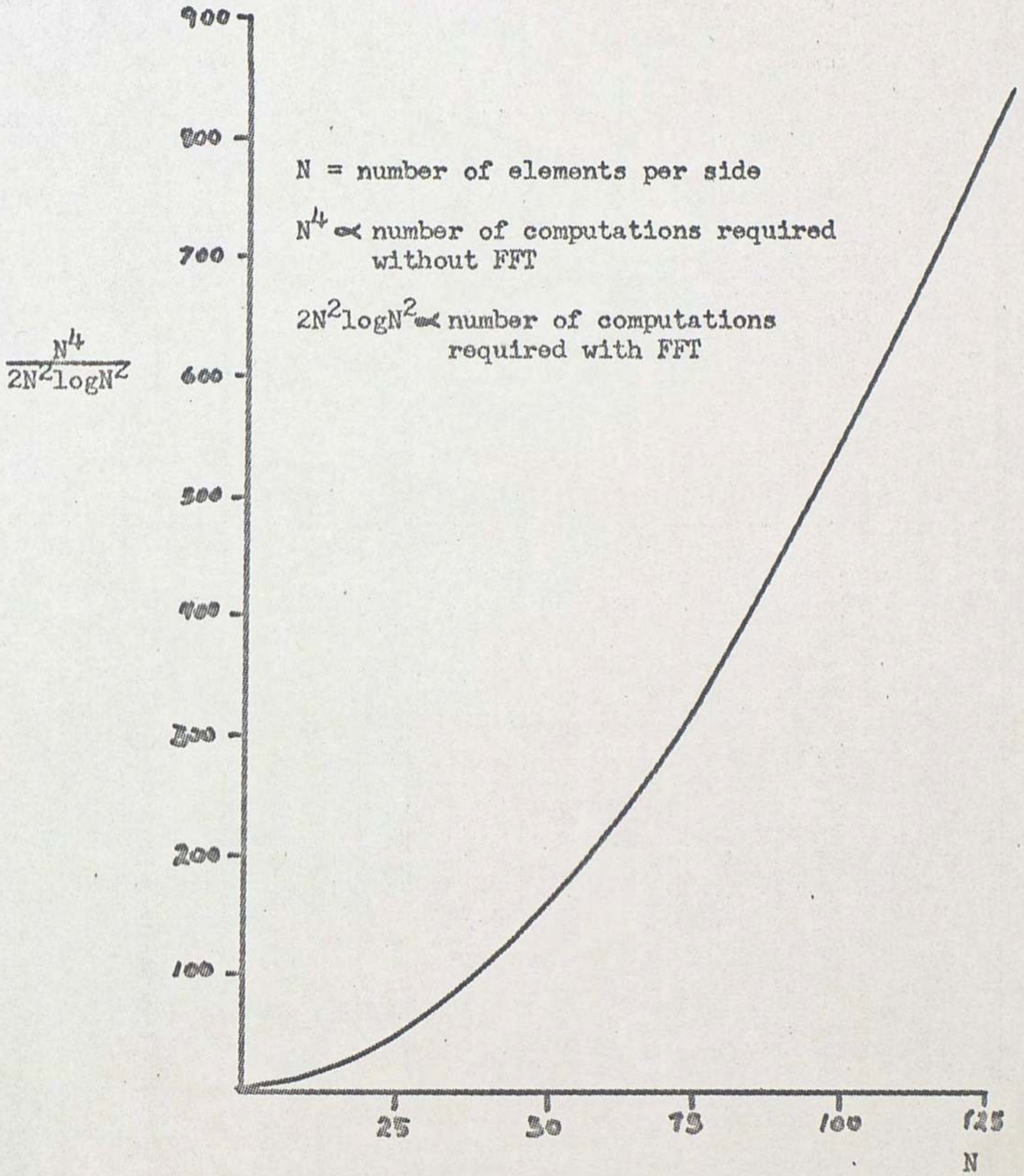

FIGURE 4: INCREASE IN COMPUTATIONAL EFFICIENCY USING THE FFT

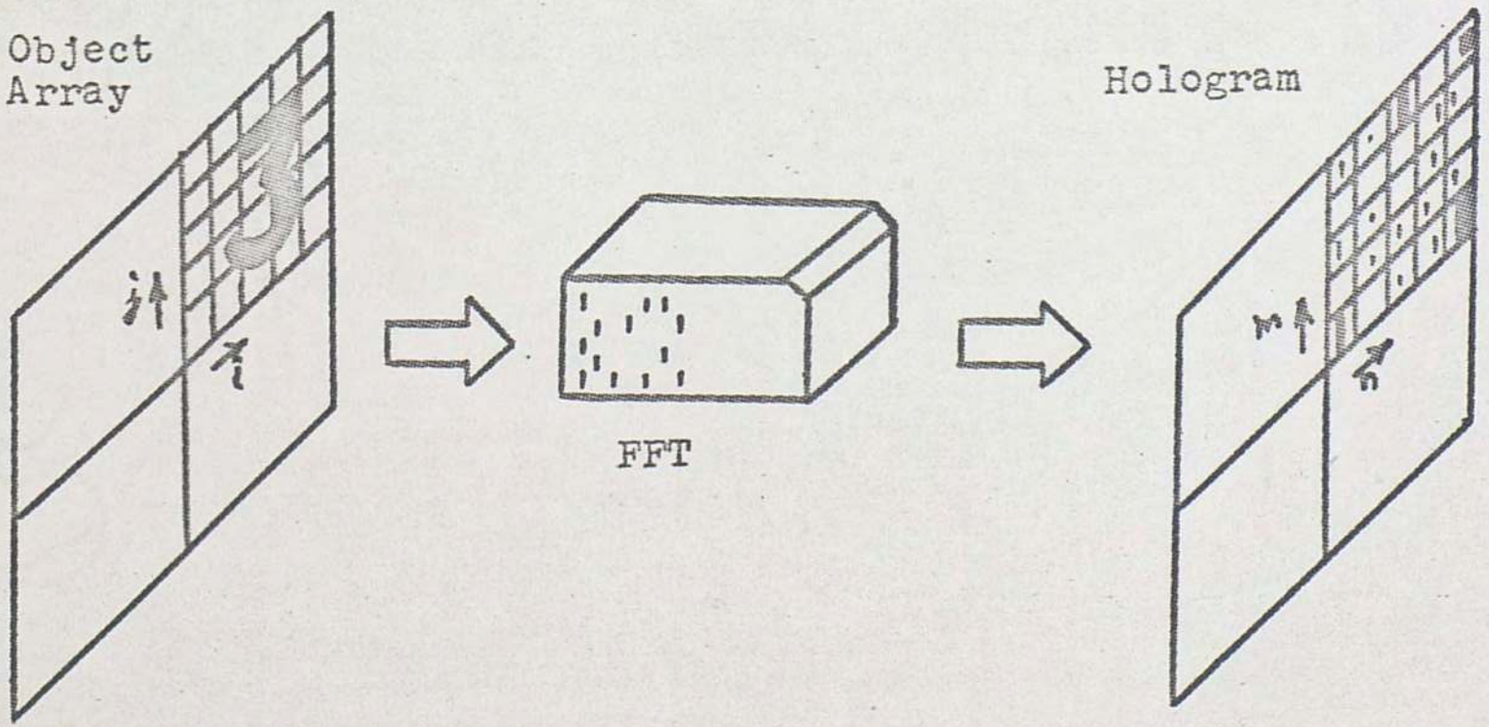

FIGURE 5: GENERATION OF A COMPUTER HOLOGRAM

in the object ranges from the center to the edge. This implies that only one fourth of the object is being transformed. In the illustration this corresponds to the numeral "3" object. Actually, the object is considered periodically extended. The transform of a single "3" in one quadrent is not calculated, rather it is implied that there is a "3" in every quadrent of the object. Also, there is more than just one transform pattern in one quadrent of the transform plane; there is a pattern in each quadrent. In order to form the total hologram, the transform obtained must be periodically extended into the three other quadrents. The object array, indicated by cross-hatching in Figure 5, is used to produce the computer generated hologram array, also indicated by cross-hatching. Extending the hologram array to the other quadrents produces the total hologram (Kronrad et. al. 1971). This format for the hologram positions the highly intense D.C. component at the center of the hologram.

When a Fast Fourier Transform subroutine transforms an object array, it returns the hologram array in a form such that each element has a real and imaginary component. This must be translated into a form that will actually produce the proper phase and amplitude when coherent radiation is incident upon the array. The amplitude transmitted by each element is proportional to the height of a rectangle in the element. The width of the rectangle is held constant. The phase variation is produced by the position of the rectangle in the array element through the use of the detour phase effect. Consider Figure 6. Figure 6a

demonstrates how an object wave without a phase shift produces a rectangular aperture in the center of the array element. Figure 6a is basically a repetition of Figure 2. While an optically produced hologram has fringes produced when the object wave is a plane wave, Figure 6a illustrates how the rectangular apertures, located in the center of the array elements, correspond to the optical fringes discussed in Figure 2. In other words, the spacing of the array elements correspond to the optical fringe spacing, and implies a given value for ℓ as given in equation 4. The array element spacing, on the other hand, is determined by the amount the hologram is photographically reduced. Note that the size of the Fourier transform of the object is always of the proper size to allow the minimum number of fringes to define it, sufficient enough to reconstruct the smallest resolvable spacing in the object. Figure 6b illustrates how the position of the rectangles are shifted when the object wave has a phase shift of $\Delta\phi$. When the phase shift is $\pm\pi$, the rectangle is located at the left or right of the array element respectively. This arrangement provides a good illustration of how the detour phase effect has an optical analogy to the fringe interference pattern produced optically when the object wave is a wave whose fringe distortion is less then $\pm\pi$. Figure 6c demonstrates how the phase shift is actually produced. At the top of the array, the reference wave is shown at such a time that the phase shift $\Delta\phi$ equals zero at the position of the transmittance aperture. At the right of the array, the positions of the apertures have been shifted by

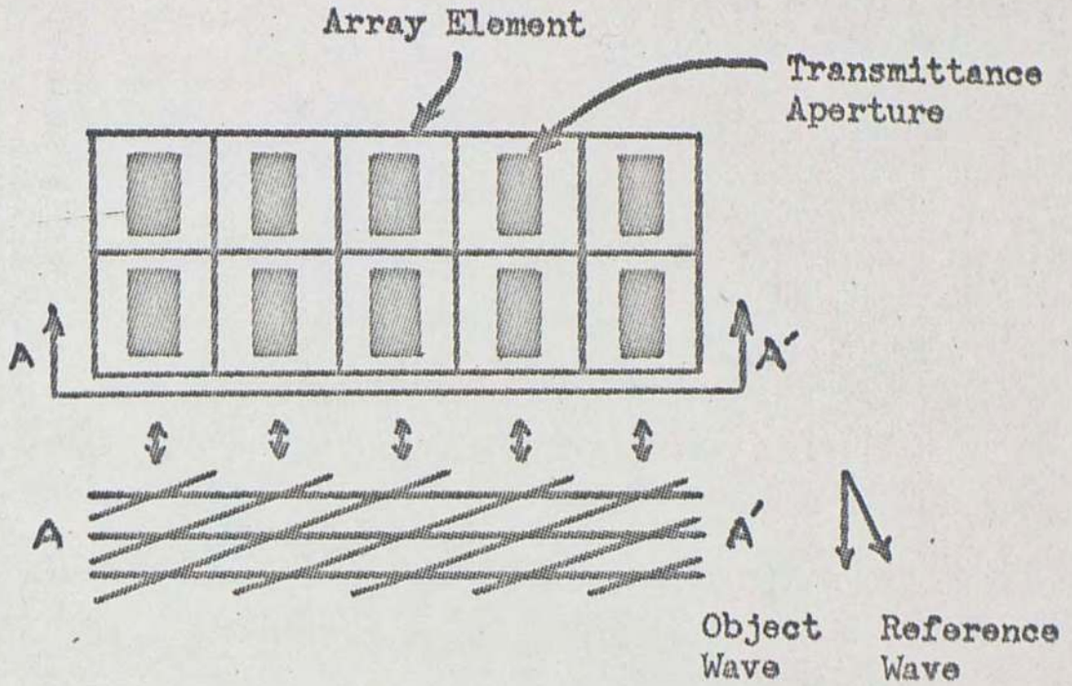

a. Object Wave Without Phase Shift

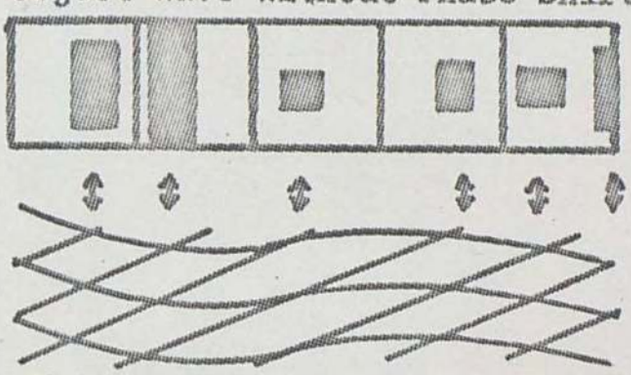

b. Object Wave With Phase Shift

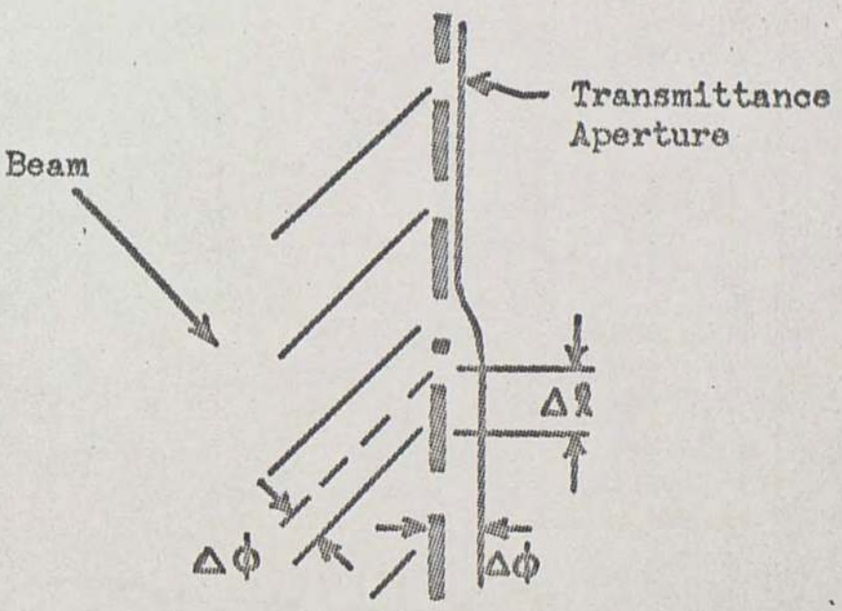

c.

FIGURE 6: DETOUR PHASE EFFECT

an amount $\Delta\ell$ so that the portion of the wave hitting these apertures has a phase of $\Delta\phi$, producing a phase shift of $\Delta\phi$ in the transmitted wave, as shown (Lohmann 1965).

The phase may vary from plus to minus π as mentioned above. If the hologram has a real and imaginary component for each element of the array, defined as:

DATAR = the real component

DATAI = the imaginary component

then the phase $\Delta\phi$ may be determined by finding the argument of the sine function,

$$\Delta\phi' = \arcsin\left(\mathrm{DATAI}/(\mathrm{DATAI}^2 + \mathrm{DATAR}^2)^{\frac{1}{2}}\right)$$

and by performing tests on the signs of the components, as illustrated in Figure 7.

The width of the rectangular aperture in an array element is roughly 1/3 of the width of the array element. This provides a good compromise between image quality and brightness.

When optical holograms are produced, they are recorded on nonlinear photographic film (See Figure 8). This has two advantages. First, if the intensity of the light falling upon the film is too high, it saturates the film. In other words, there is an intensity saturation level beyond which there is no appreciable increase in film transmissivity for a corresponding increase in light intensity. The D.C. component of the Fourier transform contains much more energy than the rest of the transform, hence the saturation effect limits the influence of the D.C. component on the final image. Second, the film has a threshold

Case I

DATAR is positive
DATAI is positive
$\Delta\phi'$ is positive

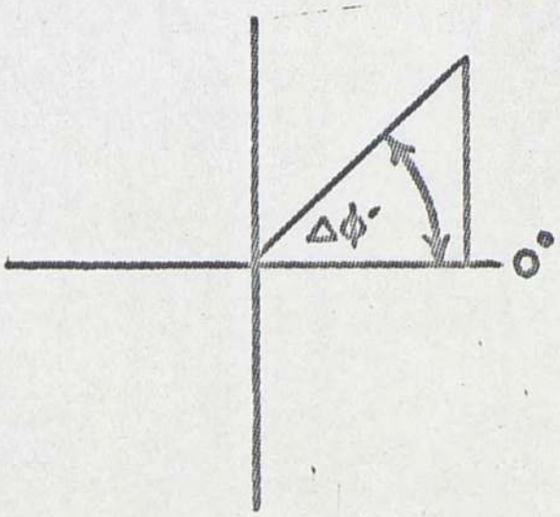

$\Delta\phi = \Delta\phi'$

Case II

DATAR is negative
DATAI is positive
$\Delta\phi'$ is positive

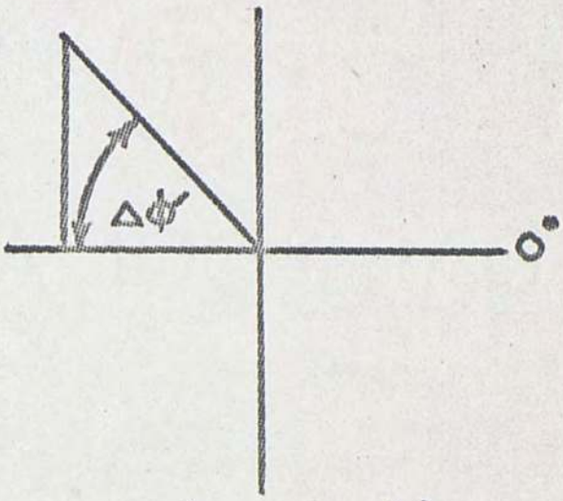

$\Delta\phi = \pi - \Delta\phi'$

Case III

DATAI is negative
DATAR is negative
$\Delta\phi'$ is negative

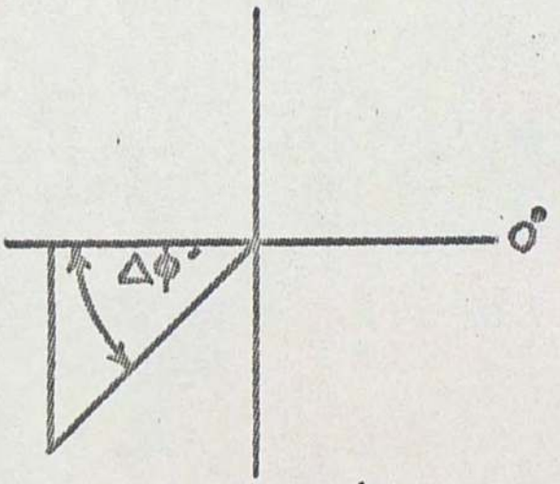

$\Delta\phi = -\pi - \Delta\phi'$

Case IV

DATAR is positive
DATAI is negative
$\Delta\phi'$ is negative

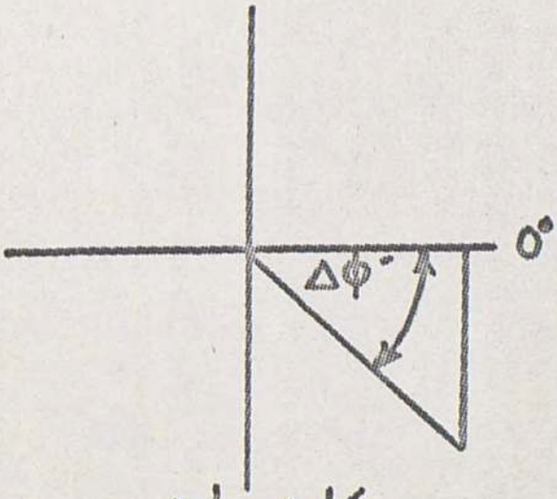

$\Delta\phi = \Delta\phi'$

$$\Delta\phi' = \arcsin \frac{DATAI}{(DATAR^2 + DATAI^2)^{\frac{1}{2}}}$$

FIGURE 7: DETERMINATION OF PHASE FROM REAL AND IMAGINARY COMPONENTS

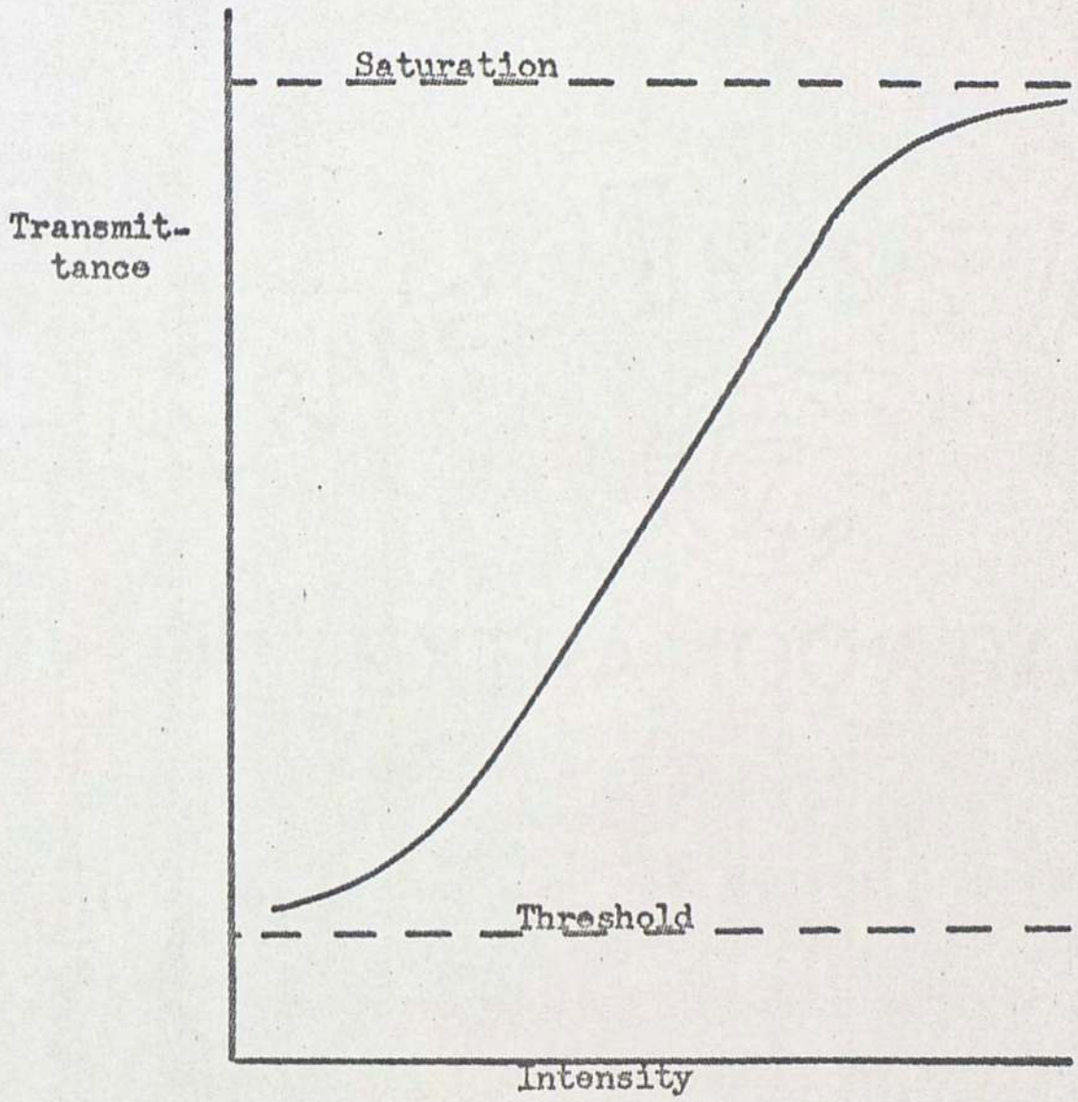

FIGURE 8: PHOTOGRAPHIC FILM NONLINEARITY

level. If the intensity of light incident upon the film is not above the threshold level, nothing is recorded on the film. This eliminates grey background noise on the hologram. These effects have been incorporated into the computer generated hologram by limiting the maximum value of the D.C. component to one third of the calculated value, and enhancing the higher frequency terms correspondingly. Terms that would produce an amplitude less than $\frac{1}{2}$ of the plotter line width are not plotted, corresponding to the film threshold effect (Lohmann and Paris, 1967).

CHAPTER IV

GENERATION OF COMPUTER HOLOGRAM AND RECONSTRUCTED IMAGE

Computer generated holograms were generated using a 64 X 64 element array. The objects were simple geometric figures without any phase distortion added.

Each element represented a real value of transmittance that varied between 0.0 and 0.9, leading to ten discrete levels of transmittance.

Typical computer run times ran from 12 to 14 seconds. Since the IBM 360/70 cost is roughly $4500 per hour, the cost per hologram is about $16. Plots were generated on a Calcomp plotter, and typically took 1½ hours to be plotted. Fortunately, there are no direct charges for the Calcomp plotter. Due to the need for a long, mistake free plot job, it is essential to have a friendly Calcomp operator, a data storage tape in good, clean condition and a program which eliminates any unnecessary pen movements. Too many pen movements in a small area can make the paper soggy. Paper fibers then stick to the pen. When the pen lifts up and moves to another location, the ink saturated fibers drag on the paper, creating an unwanted line.

The reconstruction of a circle is presented in Figure 9a.

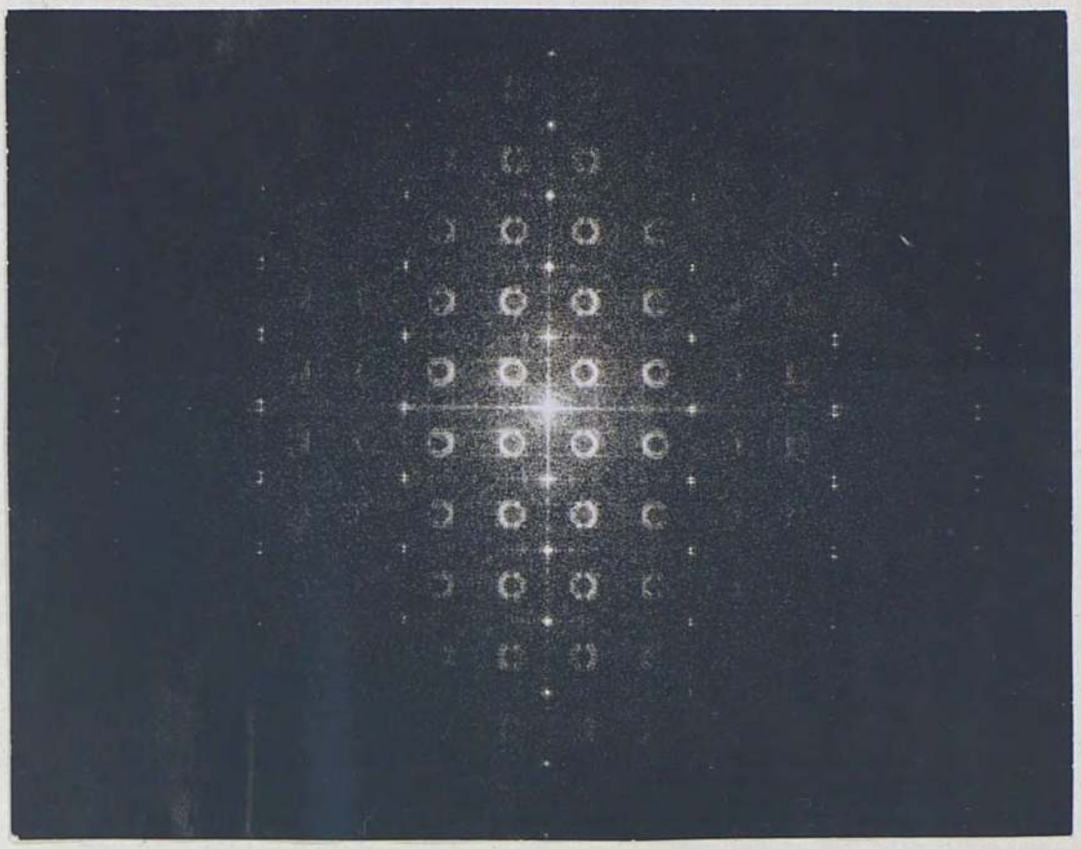

a. Reconstruction

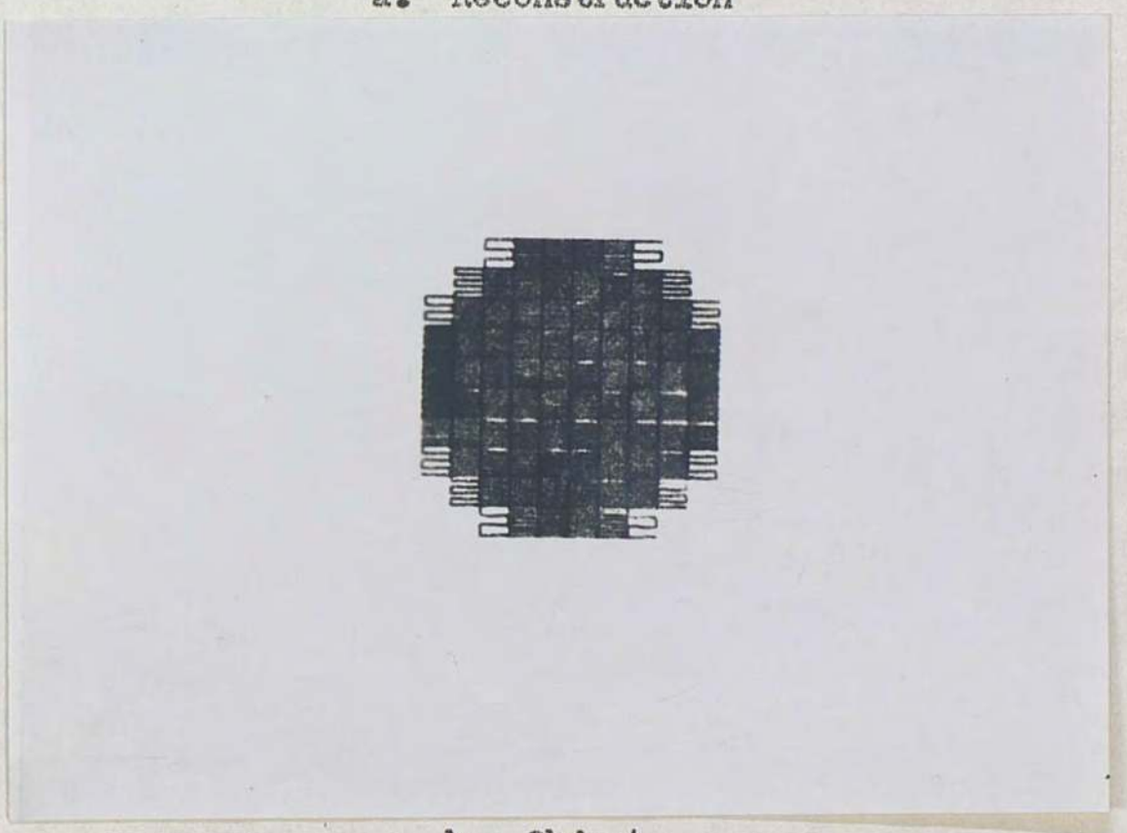

b. Object

FIGURE 9: HOLOGRAPHIC RECONSTRUCTION OF A CIRCLE

The hologram used a 32 X 32 element array and was plotted on 8 inch paper. Three seconds of computer time were used to produce the hologram. The photoreduction was performed with a 55 mm Nikkor lens apertured at F/3.5. Kodak High Contrast Copy film with a speed of ASA 64 was used. The finished hologram was 6.6 X 6.6 cm. This hologram was initially reconstructed using a 5 inch focal length lens, and a microscope was required to view the reconstruction. For Figure 9a, a 4 foot focal length lens was used and the image was recorded directly on Polaroid film. Due to the magnification achieved with the longer focal length, the image could be easily viewed through a ground glass plate. Figure 9b is a Calcomp plotter sketch of the object and is generated from the input data. These sketches are useful for verifying that the input data is correct and for comparison with the optically generated hologram. Figure 10 illustrates the actual hologram for a circle. Note in Figure 9a that the images are periodically extended, as mentioned previously.

The images are not solid circles, as expected. Only the edges show high intensity. This is probably due to the intentional suppression of the higher amplitude terms in the hologram. Since the higher amplitude terms are in the lower order elements of the hologram, this corresponds to spatial filtering by blocking the D.C. component of the hologram. This enhances the higher frequency portions of the reconstructed image at the expense of the lower frequency portions. The edges and detail in the image are brought out while the overall shading

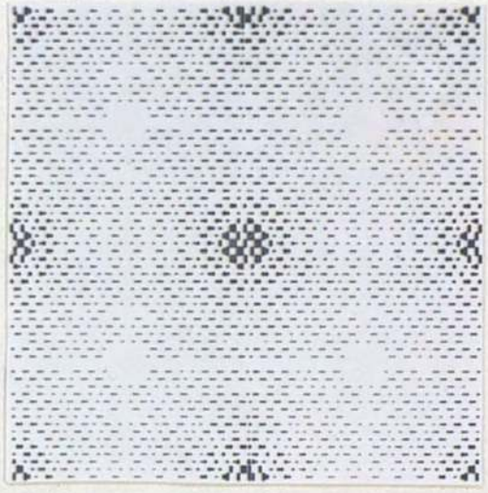

FIGURE 10: HOLOGRAM OF A CIRCLE

suffers.

The reconstruction of the number "3" is presented in Figure 11a. The hologram used 64 X 64 element array and was plotted on 26 inch paper. The production of the hologram consumed 13.2 seconds of computer time. A 20 mm Nikkor lens apertured at F/3.5 and Kodak High Contrast copy film were used for the photoreduction. This produced an 8.4 X 8.4 mm hologram. A 4 foot focal length lens was used in the reconstruction. Note the detail present in the image. Figure 11b illustrates the Calcomp plotter sketch of the object. Figure 12 is a reproduction of the hologram for the "3".

The reconstruction of the end of an optical fiber is presented in Figure 13a. The present level of development of optical fibers permits their use as practical transmission lines. It is difficult to efficiently transmit energy into the end of an optical fiber, because roughly half of the fiber face area does not transmit light. This dead region consists of the space between the fibers, which is usually filled with a binding cement. The computer generated hologram promises a method of taking a beam of light and producing a diffraction pattern which will overlap the active area on the fiber, leading to a complete utilization of the input energy. The diffraction patterns produced have sharp images which would fall perpendicularly on the fiber face. This would excite the lowest order and highest efficiency modes in the fiber. The holograms could be also easily and cheaply made. Problem areas which must be improved are the low diffraction

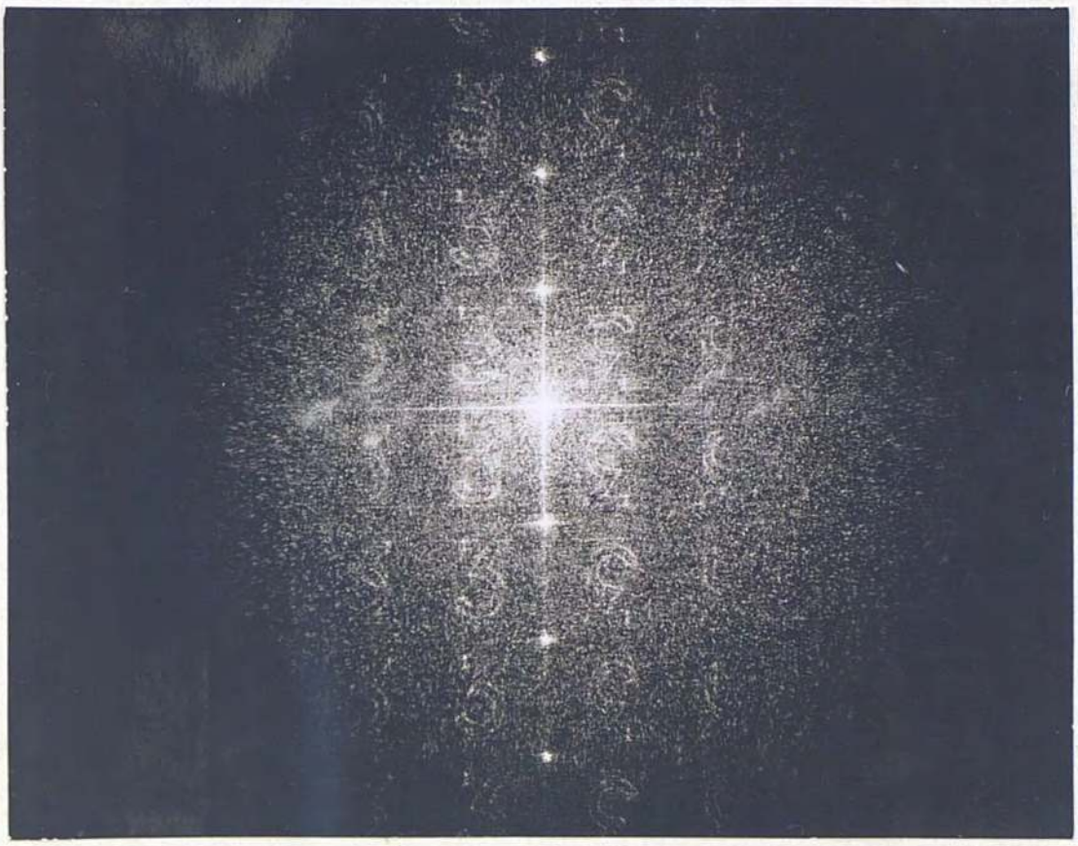

a. Reconstruction

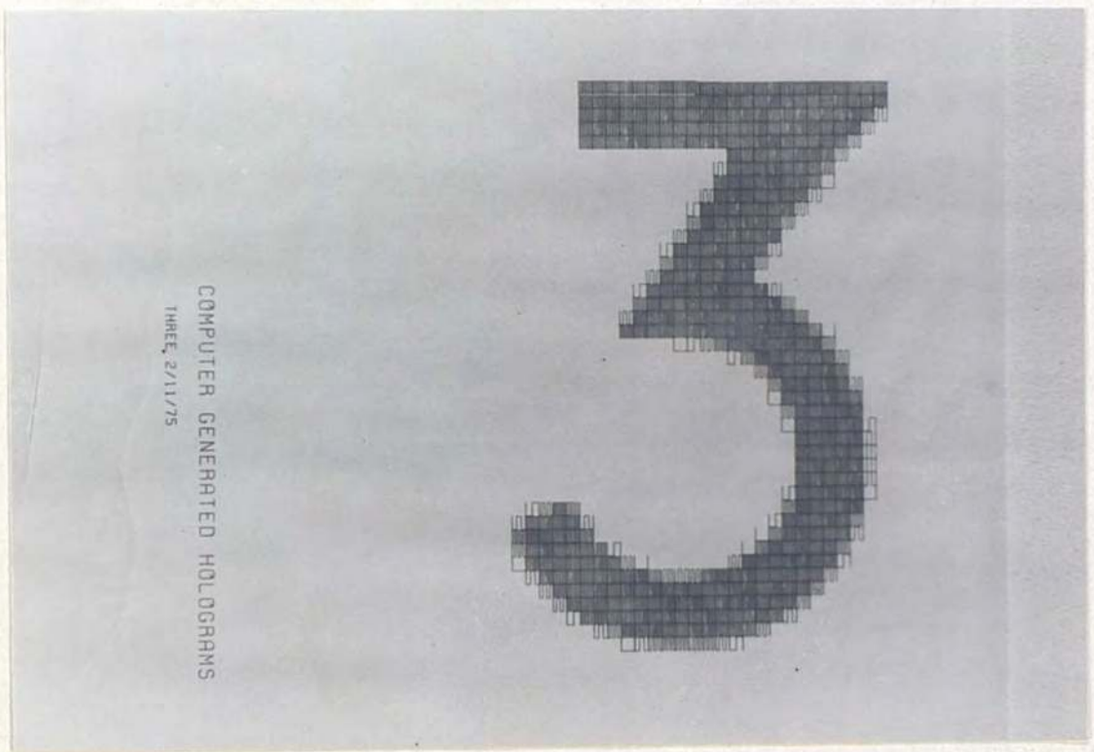

b. Object

FIGURE 11: HOLOGRAPHIC RECONSTRUCTION OF A "3"

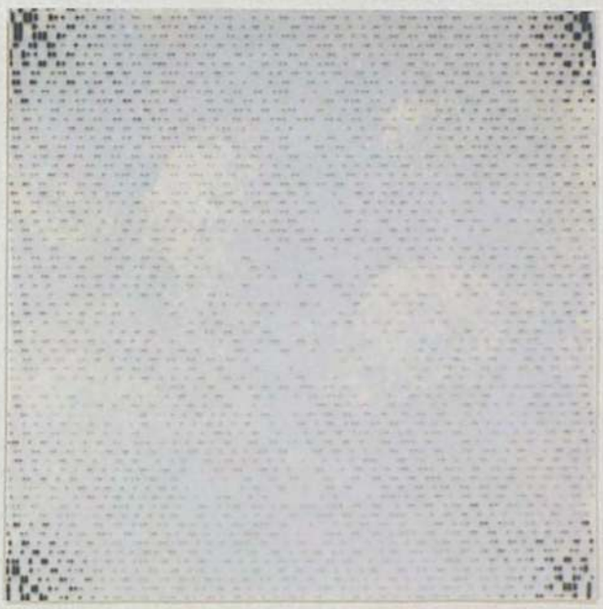

FIGURE 12: HOLOGRAM OF A "3"

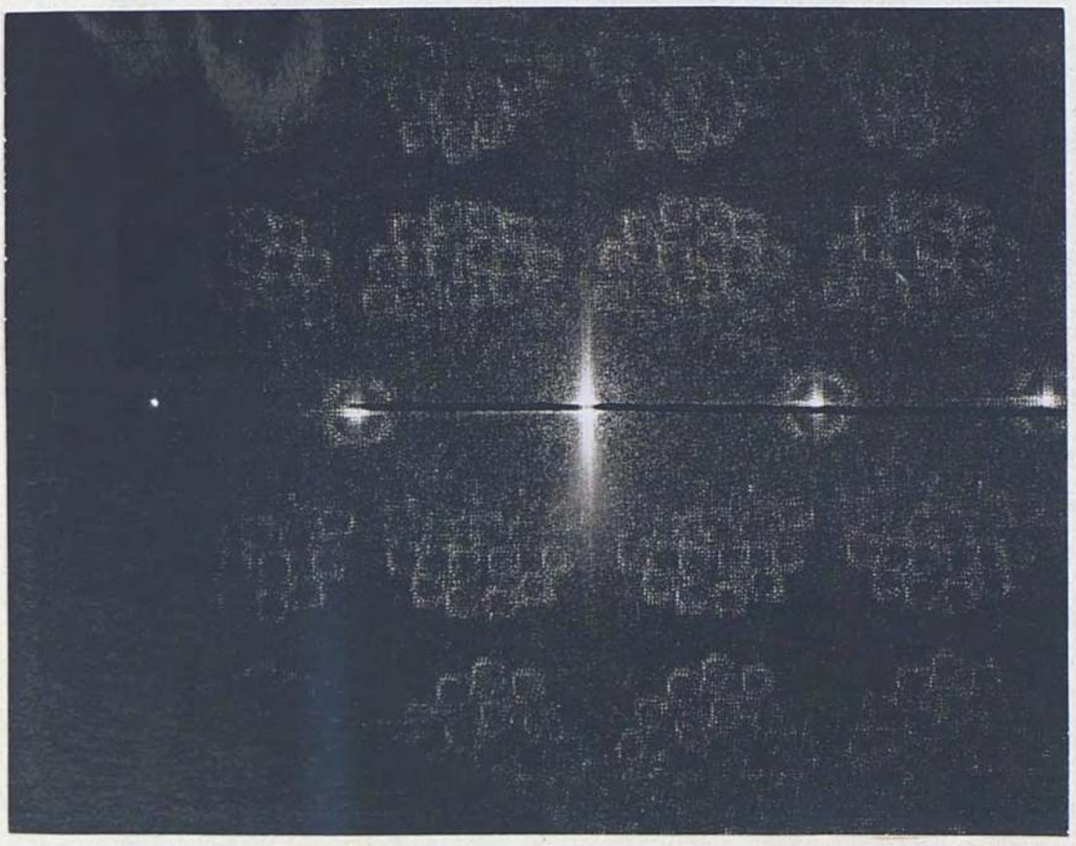

a. Reconstruction

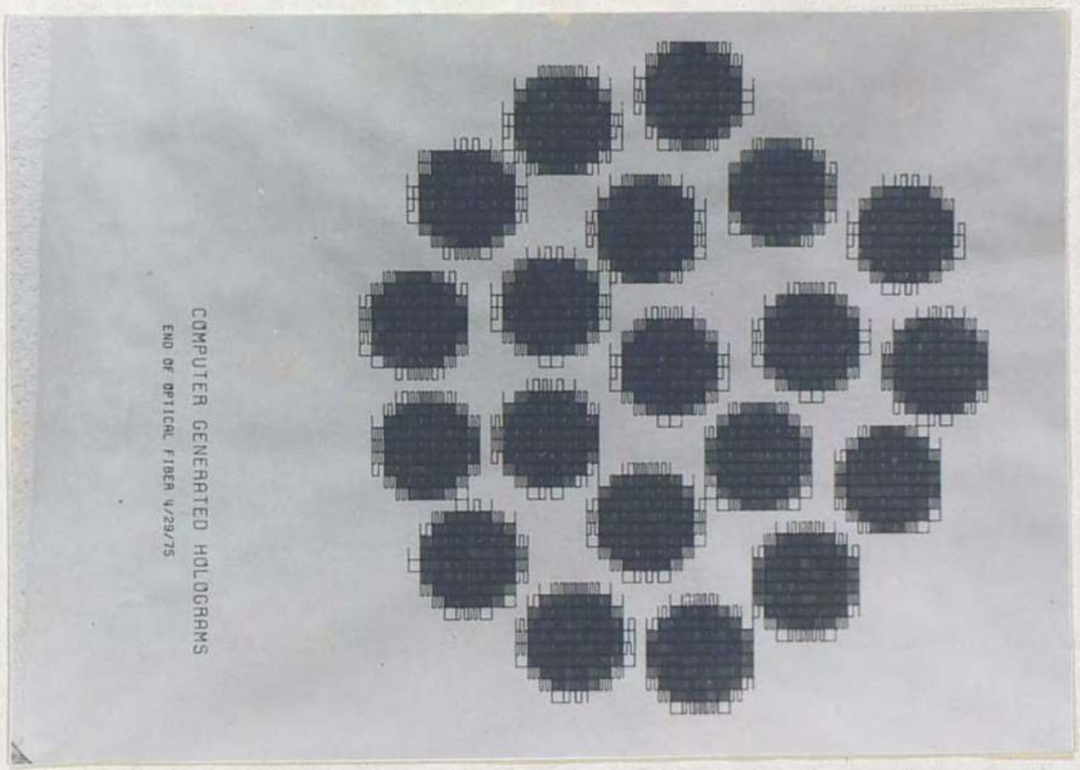

b. Object

FIGURE 13: HOLOGRAPHIC RECONSTRUCTION OF THE END OF AN OPTICAL FIBER

efficiency and repeated images. Presently most of the beam intensity is contained in the undisturbed D.C. component of the beam. Suitable methods must be found to contain most of the intensity in one diffraction image.

The hologram used a 64 X 64 element array and was plotted on 26 inch paper. The production of the hologram required 13.5 seconds of computer time. The paper plot was reduced to half size on a Xerox copy, which improved the contrast and made the job of photoreduction easier. Photoreduction was performed with a 55 mm Nikkor lens apertured at F/3.5 and Kodak Panatomic-X film with a speed of ASA 32. The finished hologram was 12.2 X 12.2 mm. A lens-mirror combination with an effective focal length of roughly 20 feet was used for the reconstruction of Figure 13a. Figure 13b is a Calcomp plot of the object. Figure 14 is a reproduction of the hologram for the optical fiber face.

FIGURE 14: HOLOGRAM OF AN OPTICAL FIBER

CHAPTER V

APPLICATIONS AND ADVANTAGES

Now that we know the details of producing computer generated holograms, and have demonstrated the ability to do so, what good does it do?

Complex wavefronts can now be defined and produced mathematically. High phase precision is now easily obtainable. There is no need for any exotic laboratory equipment, other than a laser for coherent radiation (Lee 1974). This has immediate benefits for the production and testing of spherical, parabolic, cylindrical and deformed mirrors. The forming of a surface for a mirror requires the testing of the surface of the mirror by an optical test glass, using one glass per individual surface configuration. These test glasses are produced with considerable time and expense. A computer generated hologram promises quick turn-around time from the time of need to the time of use at low cost. Some mirror surface configurations are so complex as to make the use of a test glass impossible for analysis. Then complicated interferometric analysis must be used, generally using a spherical wavefront as a reference. Analysis may be simplified by producing an exact wavefront to match the mirror surface being tested. Then the interometric fringe being analyzed

will be straight instead of complex interference patterns.

Holographic processes may be simulated and analyzed easily on the computer. The effects of altering the phase or amplitude of a portion of the hologram may be accomplished much easier on the computer rather than in the laboratory, thus being an aid to spatial filtering (Ichioka, Izumi and Suzuki). Some operations would be difficult enough as to prevent laboratory manipulations.

The very creation of a computer hologram program and a computer hologram requires considerable insight into the theory involved, and so is a valuable educational exercise.

Holograms may be created from objects that don't physically exist (Brown and Lohmann, 1969). If a complicated mathematical function is to be visually explored, a computer can plot a three dimensional projection view. If a different view is desired, the calculations must be redone. A hologram may be generated once, then different views chosen easily (Lohmann 1973).

Holograms based on different techniques than the one presented here have been produced (Chu et. al. 1973). Some of these holograms are more efficient than any previous types and some, such as the kinoform, have no physical parallel.

Improvement of lens designs can be explored through the analysis of the image, or Fourier spectrum, produced. The control and manipulation of len's image is beyond the scope of ordinary optical experiments (Ichioka et. al.).

CHAPTER VI

SUMMARY

The computer has been demonstrated to be a useful addition to the optics laboratory. The computer generated hologram is a departure from the computers traditional role of data analyzer or mathematical model performance predictor. Instead, it can now begin to step into the world of hardware, enhancing the effectiveness of some optical components, replacing entirely other components and performing some tasks that have never been performed before by conventional optical hardware. This with the added bonuses of low cost, fast turn-around time and mathematical precision.

BIBLIOGRAPHY

Brown, B.R. "Computer Synthesis of Holograms and Spatial Filters." Applications of Holography, Proceedings of the Second U.S. - Japan Seminar on Information. Washington, D.C.: IEEE, (1969).

Brown, B.R., and Lohmann, A.W. "Computer Generated Holograms." Engineering Uses of Holography. Glasgow, Scotland: IEEE, (1968).

Chu, D.C.; Fienup, J.R.: and Goodman, J.W. "Multiemulsion On-axis Computer Generated Hologram." Applied Optics. (July 1973): 1386-7.

Cooley, J.W., and Tukey, J.W. "An Algorithm for the Machine Calculation of Complex Fourier Series." Mathematics of Computation. 19 (1965): 297-301.

Gold, B., and Rader, C. Digital Processing of Signals. New York: McGraw-Hill, 1969.

Haskell, R.E., and Culver, B.C. "New Coding Technique for Computer Generated Holograms." Applied Optics. (Nov. 1972): 2712-14.

Ichioka, Y.; Izumi, M.; and Suzuki, T. "Digital Picture Processing and Holography." Applications of Holography, Proceedings of the Second U.S. - Japan Seminar on Information. Washington, D.C.: IEEE, (1969).

Kronrod, M.A.; Merzlyakov, N.S.; and Yaroslavskii, L.P. "Computer Synthesis of Transparency Holograms." Soviet-Physics-Technical Physics. Vol. 17 No. 2 (Sept. 1971): 1335-46.

Lee, W. "Binary Synthetic Holograms." Applied Optics. (July 1974): 1677-82.

Lesem, L.B.; Hirsch, P.M.; and Jordan, J.A., Jr. "Computer Generation and Reconstruction of Holograms." Proceedings of Symposium on Modern Optics. New York: Polytechnic Institute of Brooklyn, (1967).

Lohmann, A.W. "How to Make Computer Holograms." Developments in Holography, Seminar-In-Depth. Boston, Mass.: IEEE, (1965).

_____. "Computer Holography and Communications Theory." Northeast Electronics Res. and Eng. Meeting. Boston, Mass.: IEEE, (1973).

Lohmann, A.W., and Paris, D.F. "Binary Fraunhofer Holograms Generated by Computer." Applied Optics. (Oct. 1967): 1739-48.